



Contents lists available at ScienceDirect

Journal of Biomechanics

journal homepage: www.elsevier.com/locate/jbiomech
www.JBiomech.com

Gait events during turning can be detected using kinematic features originally proposed for the analysis of straight-line walking

Baptiste Ulrich^a, Alejandro N. Santos^b, Brigitte M. Jolles^{a,c}, David H. Benninger^b, Julien Favre^{a,*}^a Lausanne University Hospital and University of Lausanne (CHUV-UNIL), Department of Musculoskeletal Medicine, Swiss BioMotion Lab, Lausanne, Switzerland^b Lausanne University Hospital and University of Lausanne (CHUV-UNIL), Department of Clinical Neurosciences, Clinic of Neurology, Lausanne, Switzerland^c Ecole Polytechnique Fédérale de Lausanne (EPFL), Institute of Microengineering, Lausanne, Switzerland

ARTICLE INFO

Article history:
Accepted 5 May 2019

Keywords:
Gait analysis
Stance phase
Motion capture
Temporal parameters and turning

ABSTRACT

There is a growing interest for turning biomechanics notably because it is a more challenging task than straight-line walking during which some gait impairments are increased. Detecting heel-strike (HS) and toe-off (TO) events using the trajectory of markers attached to the feet is common in straight-line gait analysis and could reveal very useful to evaluate turning maneuvers. Yet, a comprehensive evaluation is missing, making difficult the selection of features for temporal analysis of turning. This study aimed to compare features of foot marker trajectories to detect HS and TO. Twenty healthy participants, 10 young (5 males, 23 ± 1 years old, 21.3 ± 2.2 kg/m²) and 10 elderly (4 males, 72 ± 5 years old, 26.4 ± 6.4 kg/m²), performed quarter, half, and full turns as well as straight-line walking in a gait lab. Fourteen features, adapted from straight-line walking literature, were used to detect HS and TO based on marker trajectories. Force plate measures served as reference. One HS and one TO feature were found particularly suitable. Overall, they detected more than 99% of the 1788 events recorded, with accuracies and precisions of -3.9 ms and 9.0 ms for HS and -7.8 ms and 10.7 ms for TO, respectively. Differences in accuracy and precision were observed among walking conditions and groups, but remained small, generally below 4.0 ms. In conclusion, this study identified kinematic features that can be used to analyze both turning and straight-line walking. Further assessment could be necessary with pathologies inducing severe degradation of gait patterns.

© 2019 Elsevier Ltd. All rights reserved.

1. Introduction

Although turning is an integral part of walking, representing up to half the ambulation during daily-life activities, like shopping or walking in a restaurant (Glaister et al., 2007), it was much less studied than straight-line walking. This is however changing, as turning is a more challenging task during which walking impairments and their clinical consequences could be increased. For example, in elderly, turning was associated to the risk of falling (Akram et al., 2010; Tinetti et al., 1988) and falling while turning was shown to increase the risk of hip fractures in this population (Cumming and Klineberg, 1994). Moreover, in Parkinson's disease turning was shown to be an aggravating factor for freezing of gait, a serious disabling alteration (Bhatt et al., 2013; Giladi et al., 1992; Schaafsma et al., 2003) and a risk factor for falling (Bloem et al.,

2001; Wood et al., 2002). Consequently, literature on turning biomechanics with respect to aging (Bovonsunthonchai et al., 2015; Thigpen et al., 2000) and diseases (Bhatt et al., 2013; Crenna et al., 2007; Dixon et al., 2016) is growing. This increasing interest for turning biomechanics stresses the need for methods to detect series of heel-strike (HS) and toe-off (TO) events while individuals walk along curved paths. Indeed, detecting these events is essential not only for temporal analyses of gait, but also for spatial, kinematic and electromyographic analyses.

Mainly two techniques are used to detect HS and TO during straight-line walking in a gait laboratory: stepping on a force plate (Favre et al., 2016) and identification of particular features in foot kinematic signals (Bennour et al., 2018; Barrios et al., 2010). The first technique is hardly compatible with the detection of series of gait events during turning because it would require each foot-step to occur on a single force plate and to have only one foot on one force plate at a time. Since turning maneuvers often consist in small steps (Huxham et al., 2006; Strike and Taylor, 2009), this technique would require many force plates arranged following layouts that may need to be changed between individuals and

* Corresponding author at: Lausanne University Hospital (CHUV), Department of Musculoskeletal Medicine (DAL), Hôpital Nestlé – Office NES/03/3015, Avenue Pierre-Decker 5, CH-1011 Lausanne, Switzerland.

E-mail address: julien.favre@chuv.ch (J. Favre).

walking conditions. On the contrary, the kinematics-based approach is particularly attractive because it could allow the monitoring of series of HS and TO, without having to constrain the gait by requesting the subjects to step on specific locations or follow particular paths. Furthermore, this second technique is compatible with the trajectory data provided by marker-based motion capture systems frequently available in gait laboratories, thus avoiding the purchase of additional equipment solely for the temporal analysis of turning.

Different authors have proposed features of foot marker trajectories to detect HS and TO (Desailly et al., 2009; Ghoussayni et al., 2004; Hreljac and Marshall, 2000; Hsue et al., 2007; O'Connor et al., 2007; Salazar-Torres, 2006; Zeni et al., 2008). Studies were even conducted to compare the features during straight-line walking and concluded that combining features proposed by different authors could improve the detections (Bruening and Ridge, 2014;

Hendershot et al., 2016). However, these features were designed for straight-line walking and needed to be extended for turning maneuvers. Furthermore, a comprehensive evaluation during turning was necessary to guide the selection of the features to analyze curved paths.

This study aimed at comparing features of foot marker trajectories to detect HS and TO during turning in terms of capacity to detect the events and of accuracy and precision of the detected events. In accordance with the interest expressed for turning biomechanics in literature (Bourgeois et al., 2014; Mellone et al., 2016; Orendurff et al., 2006; Strike and Taylor, 2009; Taylor et al., 2005), the comparisons were done with young and elderly adults performing turns of 90° , 180° and 360° . Since some features were described only in the context of straight-line walking, a secondary objective of this study was to adapt them to turning maneuvers.

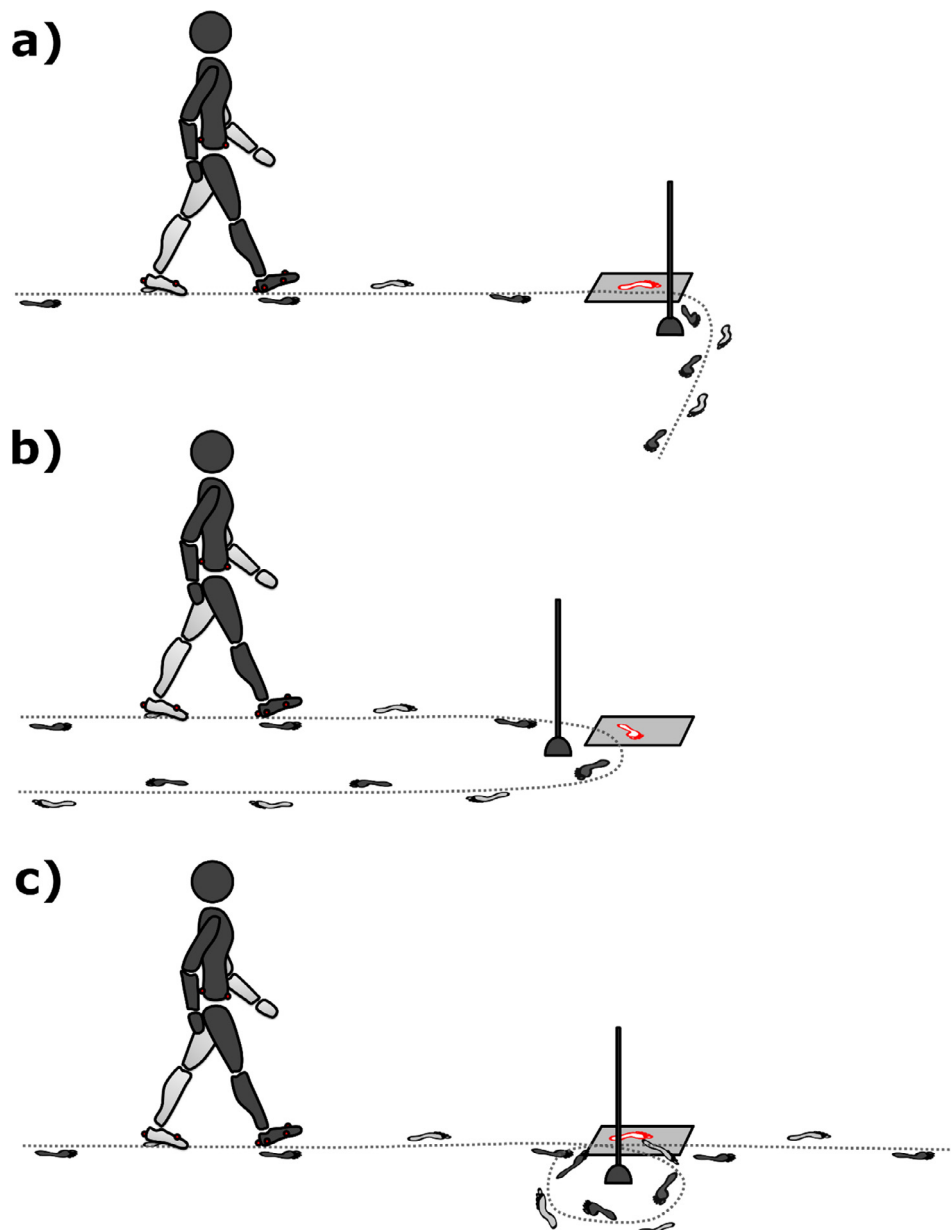


Fig. 1. Illustration of the three turning amplitudes: (a) quarter turn (90°), (b) half turn (180°), and (c) full turn (360°). This figure also illustrates the initiation (a), middle (b) and end (c) stages of the turn during which HS and TO detections were assessed.

2. Method

2.1. Participants

Twenty healthy subjects were enrolled in this IRB-approved study after providing written consent. They were composed of 10 young (5 males, 23 ± 1 years old, 21.3 ± 2.2 kg/m²) and 10 elderly (4 males, 72 ± 5 years old, 26.4 ± 6.4 kg/m²) adults.

2.2. Experimental protocol

Participants were out-fitted with reflective markers on both feet and on the pelvis. Markers were placed as described in prior studies proposing methods to detect HS and TO based on foot kinematics (Desailly et al., 2009; Ghousayni et al., 2004; Hreljac and Marshall, 2000; Hsue et al., 2007; O'Connor et al., 2007; Salazar-Torres, 2006; Zeni et al., 2008). Specifically, foot markers were attached to the posterior side of calcaneus, the lateral side of calcaneus, the second metatarsal heads and the fifth metatarsal heads. Pelvis markers were attached to both anterior superior iliac spines and both posterior superior iliac spines.

Participants then performed straight-line and turning walking trials barefoot in a lab equipped with a motion capture system (Vicon, Oxford, UK) and floor-embedded force plates (Kistler AG, Winterthur, CH). Cameras and force plates data were recorded synchronously at 120 Hz and 1200 Hz, respectively. The straight-line trials consisted of 10 m of straight walking. Trials with a single-foot stance on a force plate were recorded for analysis. For the turning trials, participants were asked to walk 5 m straight, turn around a vertical rod and continue walking straight for at least

3 m (Fig. 1). Three turning amplitudes were tested: quarter-turn (90°), half-turn (180°) and full-turn (360°). Moreover, for each amplitude, the HS and TO detections were assessed for three stages: initiation, middle, and end of the turn (Fig. 1). Initiation and end stages were defined as the last steps posterior and the first steps anterior to the rod, respectively (Fig. 1). Middle stage corresponded to steps in between. Similar to straight-line walking, trials with a single-foot stance on a force plate were recorded for analysis. One stance on a force plate, either at initiation, middle or end of the turn, was analyzed per trial. The vertical rod was moved between trials to facilitate the recording of the nine turning conditions (3 amplitudes \times 3 stages) (Fig. 1). The conditions were tested in randomized order. Furthermore, a turning direction (left or right) was defined randomly for each participant and all the trials of that individual were collected for this direction. Walking conditions were demonstrated to help participants understand where to start, how much to turn and where to finish. Three trials per condition were recorded for each participant walking at self-selected normal speed. Three additional trials per condition were also recorded for the young participants while they walked at self-selected slower than normal speed. None of the speed was controlled.

2.3. Heel-strike and toe-off detection

For each trial, reference HS and TO times were determined by thresholding the vertical force of the force plate at 10 N. Force plate thresholding is considered the gold standard to detect HS and TO (Hreljac and Marshall, 2000; O'Connor et al., 2007; Zeni et al., 2008).

Table 1

Summary of the marker sets and kinematic features used to detect HS and TO.

Methods	Markers	HS features	TO features
O'Connor (O'Connor et al., 2007)	Posterior side of the calcaneus Second metatarsal head	Peak of downward vertical ^a velocity of a virtual marker located at the middle of the posterior calcaneus & second metatarsal head markers	Maximum upward vertical ^a velocity of a virtual marker located at the middle of the posterior calcaneus & second metatarsal head markers
Hreljac (Hreljac and Marshall, 2000) ^f	Lateral side of the calcaneus Fifth metatarsal head Superior iliac spines ^e	Peak of upward vertical ^a acceleration of the lateral calcaneus marker	Maximum anterior ^b acceleration of the fifth metatarsal head marker
Ghousayni ^d (Ghousayni et al., 2004)	Lateral side of the calcaneus Fifth metatarsal head Superior iliac spines ^e	Threshold on sagittal-plane velocity ^c of the lateral calcaneus marker	Threshold on sagittal-plane velocity ^c of the fifth metatarsal head marker
Zeni (Zeni et al., 2008) ^g	Posterior side of the calcaneus Second metatarsal head Posterior superior iliac spines Anterior superior iliac spines ^e	Maximum anterior ^b position of the posterior calcaneus marker compared to the position of a virtual sacrum marker located at the middle of the left and right posterior superior iliac spine markers	Maximum posterior ^b position of the second metatarsal head marker compared to the position of a virtual sacrum marker located at the middle of the left and right posterior superior iliac spine markers
Desailly (Desailly et al., 2009)	Posterior side of the calcaneus Second metatarsal head Superior iliac spines ^e	Maximum anterior ^b high-pass filtered position of the posterior calcaneus or second metatarsal head markers (first between the two)	Maximum posterior ^b high-pass filtered position of the posterior calcaneus or second metatarsal head markers (first of the two)
Salazar-Torres (Salazar-Torres, 2006)	Second metatarsal head Superior iliac spines ^e	Threshold on the ratio between the anterior ^b velocity and the sagittal-plane velocity ^c of the second metatarsal head marker	Threshold on the ratio between the anterior ^b velocity and the sagittal-plane velocity ^c of the second metatarsal head marker
Hsue (Hsue et al., 2007)	Second metatarsal head Superior iliac spines ^e	Maximum posterior ^b acceleration of the second metatarsal head marker	Maximum anterior ^b acceleration of the second metatarsal head marker

^a Vertical axis of the lab for both straight-line and turning trials.

^b During straight-line trials, the anterior-posterior axis was collinear to the walkway axis of the lab. For turning trials, the methods were modified to use the tangent to the pelvis trajectory in the horizontal plane of the lab as the anterior-posterior axis. During turning, the anterior-posterior axis varied continuously over time. The pelvis trajectory was defined as the movement of a virtual marker at the middle of the four superior iliac spine markers (see subscript letter: e).

^c The sagittal-plane velocities were defined as the resultant of antero-posterior^b and vertical^a velocities.

^d Thresholds were modified from the original publication and set at 500 mm/s for HS and TO (Bruening and Ridge, 2014).

^e Markers added to the original methods to determine the trajectory of the pelvis during turning. These markers are not necessary for straight-line walking.

^f The original description of the method does not specify the placement of the heel marker. This marker was placed following a subsequent publication of the first author (Hreljac and Stergiou, 2000).

^g The original description of the method does not specify the placement of the heel marker. This marker was placed following a subsequent publication of the first author (Zeni and Higginson, 2010).

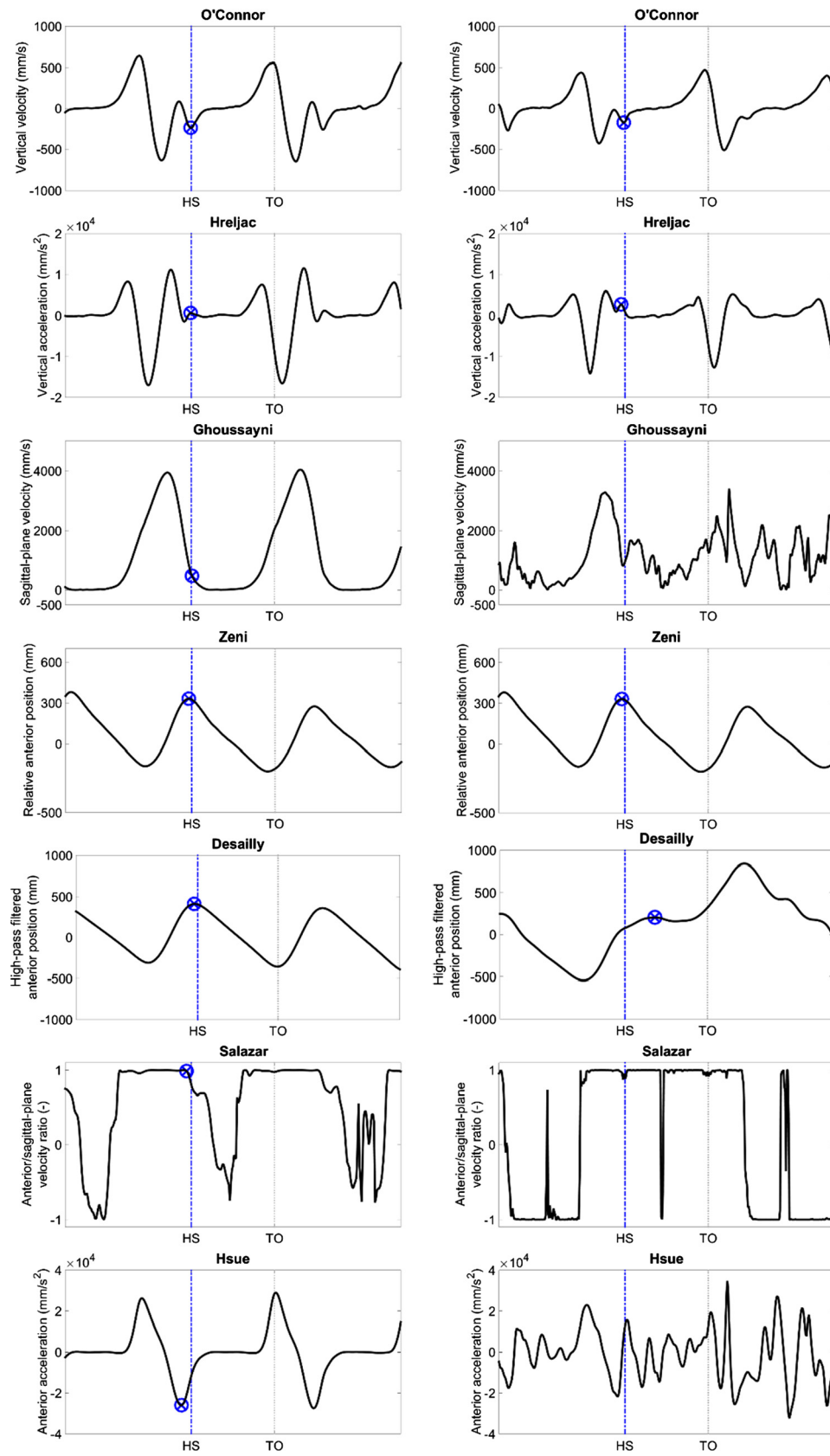


Fig. 2. Typical examples of the kinematic signals used by the seven methods for HS detection. The left column reports signals during straight-line walking, and the right column during the middle stage of a full turn. This figure also reports the HS times detected by the force plates (blue dashed lines) and the kinematic features (blue marks). The absence of blue mark indicates that no HS could be detected because the feature of interest could not be identified. (For interpretation of the references to colour in this figure legend, the reader is referred to the web version of this article.)

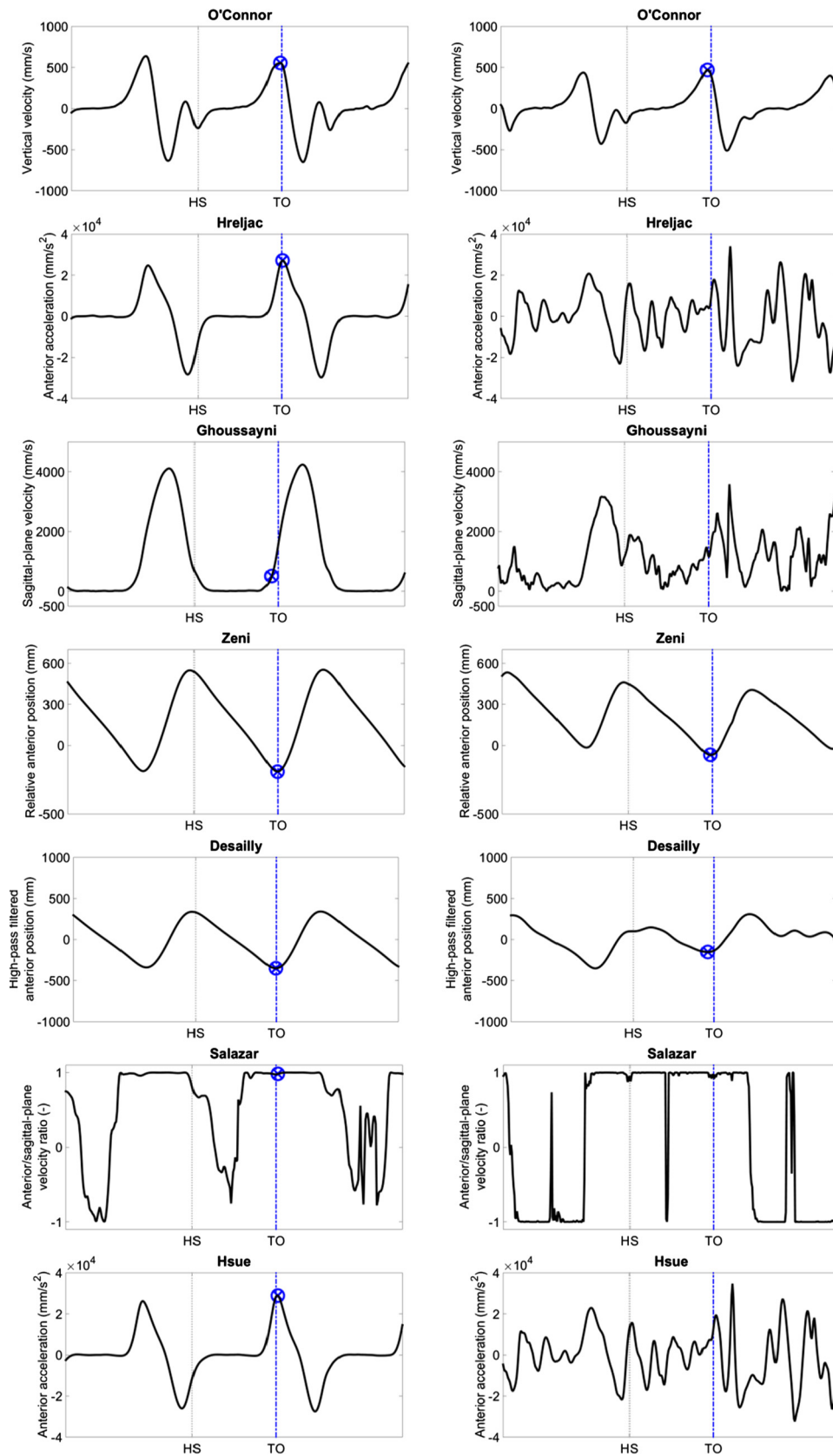


Fig. 3. Typical examples of the kinematic signals used by the seven methods for TO detection. The left column reports signals during straight-line walking, and the right column during the middle stage of a full turn. This figure also reports the TO times detected by the force plates (blue dashed lines) and the kinematic features (blue marks). The absence of blue mark indicates that no TO could be detected because the feature of interest could not be identified. (For interpretation of the references to colour in this figure legend, the reader is referred to the web version of this article.)

Seven methods to detect gait events based on foot marker trajectories were identified in literature (Desailly et al., 2009; Ghoussayni et al., 2004; Hreljac and Marshall, 2000; Hsue et al., 2007; O'Connor et al., 2007; Salazar-Torres, 2006; Zeni et al., 2008), with one of them using a combination of foot and posterior superior iliac spine markers (Zeni et al., 2008). Consequently, seven HS and seven TO features of marker trajectories were analyzed. For convenience, they are named after the first author's last name written in *italic*. Eleven features were originally described using kinematic signals calculated based on the walkway axis of the lab (Desailly et al., 2009; Ghoussayni et al., 2004; Hreljac and Marshall, 2000; Hsue et al., 2007; Salazar-Torres, 2006; Zeni et al., 2008). While appropriate for straight-line walking, this approach needed to be adapted to the curved paths of turning maneuvers. The adaptation was done by calculating the “anterior-posterior” signals, originally parallel to the walkway axis, as tangent to pelvis trajectory in the horizontal plane of the lab. The pelvis trajectory was defined as the movement of a virtual marker at the middle of the four superior iliac spine markers. Similarly, the “sagittal-plane” signals, originally in a plane based on the walkway and lab vertical axes, were calculated using a plane defined by the new anterior-posterior axis defined above and the vertical axis of the lab. With these adaptations, the anterior-posterior and sagittal-plane kinematic signals were expressed relative to frames that varied continuously over time during the turning trials, following participant trajectories. Specific features associated with HS and TO were then detected in these kinematic signals, as previously described. The features are summarized in Table 1 and illustrated in Figs. 2 and 3. Automatic detection algorithms were implemented following prior publications as faithfully as possible. The only exception was with *Ghoussayni*, for which thresholds set at 500 mm/s (instead of 50 mm/s) were used for HS and TO detections, as proposed by Bruening and Ridge (2014). Since automatic detection of some features could be difficult during turning trials, every trial was visually checked and manually corrected when necessary so they matched the definitions in Table 1. This post-checking was done to allow the comparison of the relevance of the features independently of the quality of the detection algorithms. When a feature was not present in a signal, it was noted that the method failed to detect the event.

2.4. Statistical analysis

The 14 features were first assessed in terms of their capacity to detect the events. To this end, the percentage of detection (i.e., number of events detected relative to the number of events recorded) was computed per feature, walking condition and group (young participants walking at normal speed, young participants at slower speed and elderly participants at normal speed). Each percentage was based on 30 stance phases (one per trial; 3 trials per participant), except for middle stage of full-turn of the elderly group where it was based on 24 stances (8 participants), as two participants had too short stride lengths to record clear steps on a force plate. In addition, the overall percentage of detection, without distinction for walking conditions and groups, was calculated based on the 894 stances recorded in this study.

Only the features with more than 80% of detection percentage for every walking condition and group were considered possibly suitable for further uses, and their accuracies and precisions were computed. To this end, time errors were calculated for each stance phase by comparing the times when the kinematics-based methods and the reference method (force plate) detected the events. Negative/positive errors indicate that the kinematics-based method detected the event before/after the reference method. Kolmogorov-Smirnov tests indicated that the time errors were normally distributed and 3-way ANOVAs, performed separately for

each feature, indicated that the time errors during turning maneuvers differed with respect to the group, the amplitude and the stage of the turn. Consequently, the time errors were reported in terms of accuracy (mean) and precision (standard deviation) per walking condition and group. Similar to the calculation of the detection percentages above, each accuracy and precision value was based on 30 stance phases, except for middle stage of full-turn of the elderly group where it was based on 24 stances. Finally, to determine if the accuracies differed among features, one-way repeated ANOVAs were performed per type of event, walking condition and group. When necessary, post-hoc paired t-tests were used to compare the features. If two features were found to be different in post-hoc analyses, the mean values of the absolute time errors were calculated for both features and the feature with the smallest value was considered the most accurate of the two. Doing so allowed identifying the most accurate features even when negative and positive accuracies were compared. Additionally, to test whether the precisions were different among features, Bartlett tests were performed per type of event, walking condition and group. When appropriate, post-hoc two-sample F-tests were done to compare the feature precisions. Statistical significance level was set *a-priori* at 0.05, with Bonferroni adjustment for multiple comparisons in post-hoc analyses. Signal processing and statistics were done with Matlab version 2014b (Mathworks, Natick, MA).

3. Results

The mean (\pm standard deviation) gait velocity was 1.14 ± 0.11 m/s for the young participants walking at normal speed, 0.89 ± 0.14 m/s for the young participants at slower speed and 0.96 ± 0.11 m/s for the elderly participants at normal speed. Although this study recoded straight-line walking and multiple turning manoeuvres in diverse persons and at different speeds, there was a consistent pattern of vertical ground reaction force during stance phase (Fig. 4).

The percentages of HS and TO detection for straight-line walking were of 100% for all features and groups, except for *Hreljac* HS feature in the elderly group, where it was of 93% (Table 2). During turning trials, *O'Connor*, *Zeni* and *Desailly* features showed HS and TO detection percentages above 80% for all conditions and groups. Specifically, *Zeni* detected all HS and TO, whereas *O'Connor* and *Desailly* detected all TO, but missed some HS (overall percentage above 99%). The eight other features had inconsistent detection

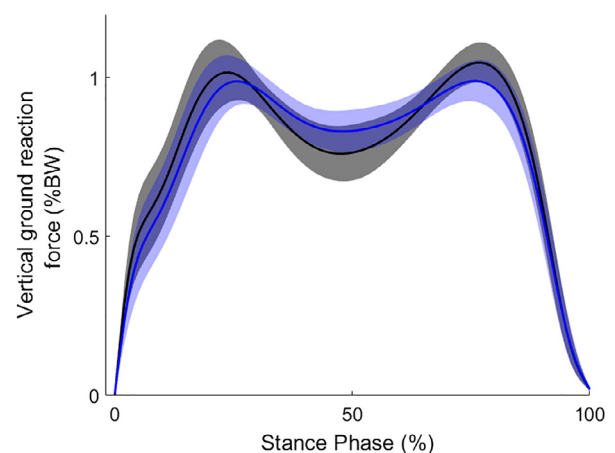


Fig. 4. Vertical ground reaction force during stance phase for straight-line walking (dark gray) and turning manoeuvres (blue). The lines and shaded areas correspond to the averages and standard deviations over all trials, respectively. Forces are expressed in percentage of body weight (%BW). (For interpretation of the references to colour in this figure legend, the reader is referred to the web version of this article.)

Table 2
Percentage of heel-strike (HS) and toe-off (TO) detection per feature, walking condition and group.

Group	Walking condition	<i>O'Connor</i>		<i>Hreljac</i>		<i>Ghoussayni</i>		<i>Zeni</i>		<i>Desailly</i>		<i>Salazar</i>		<i>Hsue</i>	
		HS (%)	TO (%)	HS (%)	TO (%)	HS (%)	TO (%)	HS (%)	TO (%)	HS (%)	TO (%)	HS (%)	TO (%)	HS (%)	TO (%)
Young normal walking speed	Straight-line	100.0	100.0	100.0	100.0	100.0	100.0	100.0	100.0	100.0	100.0	100.0	100.0	100.0	100.0
	90-I	100.0	100.0	100.0	73.3	96.7	73.3	100.0	100.0	100.0	100.0	100.0	100.0	100.0	76.7
	90-M	100.0	100.0	100.0	90.0	100.0	90.0	100.0	100.0	100.0	100.0	86.7	66.7	96.7	100.0
	90-E	100.0	100.0	100.0	90.0	100.0	100.0	100.0	100.0	100.0	100.0	86.7	70.0	86.7	96.7
	180-I	100.0	100.0	96.7	56.7	93.3	56.7	100.0	100.0	100.0	100.0	100.0	83.3	100.0	53.3
	180-M	100.0	100.0	83.3	73.3	36.7	63.3	100.0	100.0	100.0	100.0	46.7	63.3	73.3	86.7
	180-E	100.0	100.0	86.7	86.7	90.0	96.7	100.0	100.0	100.0	100.0	16.7	46.7	76.7	96.7
	360-I	100.0	100.0	100.0	63.3	100.0	56.7	100.0	100.0	100.0	100.0	76.7	86.7	100.0	60.0
	360-M	100.0	100.0	82.8	44.8	41.4	37.9	100.0	100.0	100.0	100.0	27.6	34.5	41.4	41.4
	360-E	100.0	100.0	70.0	90.0	80.0	100.0	100.0	100.0	100.0	100.0	80.0	86.7	86.7	96.7
Young slower walking speed	Straight-line	100.0	100.0	100.0	100.0	100.0	100.0	100.0	100.0	100.0	100.0	100.0	100.0	100.0	100.0
	90-I	100.0	100.0	100.0	66.7	100.0	80.0	100.0	100.0	100.0	100.0	96.7	86.7	96.7	66.7
	90-M	100.0	100.0	100.0	93.3	100.0	86.7	100.0	100.0	100.0	100.0	96.7	56.7	90.0	90.0
	90-E	100.0	100.0	100.0	96.7	96.7	100.0	100.0	100.0	100.0	100.0	86.7	60.0	83.3	100.0
	180-I	100.0	100.0	93.3	60.0	100.0	60.0	100.0	100.0	100.0	100.0	86.7	56.7	93.3	53.3
	180-M	100.0	100.0	93.3	66.7	46.7	80.0	100.0	100.0	100.0	100.0	46.7	60.0	53.3	86.7
	180-E	100.0	100.0	83.3	86.7	93.3	100.0	100.0	100.0	100.0	100.0	36.7	46.7	60.0	86.7
	360-I	100.0	100.0	100.0	56.7	93.3	56.7	100.0	100.0	100.0	100.0	76.7	60.0	86.7	66.7
	360-M	100.0	100.0	93.3	46.7	53.3	56.7	100.0	100.0	93.3	100.0	36.7	36.7	50.0	76.7
	360-E	100.0	100.0	93.3	96.7	86.7	100.0	100.0	100.0	100.0	100.0	56.7	76.7	93.3	96.7
Elderly normal walking speed	Straight-line	100.0	100.0	93.3	100.0	100.0	100.0	100.0	100.0	100.0	100.0	100.0	100.0	100.0	100.0
	90-I	100.0	100.0	93.3	93.3	100.0	93.3	100.0	100.0	100.0	100.0	96.7	93.3	96.7	96.7
	90-M	100.0	100.0	93.3	86.7	100.0	100.0	100.0	100.0	100.0	100.0	93.3	83.3	100.0	90.0
	90-E	100.0	100.0	83.3	90.0	96.7	96.7	100.0	100.0	100.0	100.0	80.0	80.0	80.0	96.7
	180-I	100.0	100.0	96.7	100.0	100.0	100.0	100.0	100.0	100.0	100.0	93.3	60.0	100.0	93.3
	180-M	96.7	100.0	80.0	73.3	46.7	60.0	100.0	100.0	100.0	100.0	56.7	60.0	70.0	70.0
	180-E	96.7	100.0	80.0	80.0	90.0	100.0	100.0	100.0	96.7	100.0	83.3	76.7	66.7	93.3
	360-I	100.0	100.0	93.3	93.3	96.7	96.7	100.0	100.0	100.0	100.0	100.0	86.7	96.7	90.0
	360-M	95.8	100.0	58.3	66.7	45.8	75.0	100.0	100.0	83.3	100.0	41.7	62.5	45.8	75.0
	360-E	100.0	100.0	80.0	80.0	93.3	100.0	100.0	100.0	100.0	100.0	66.7	100.0	86.7	96.7
Overall		99.7	100.0	91.2	80.2	86.2	84.0	100.0	100.0	99.2	100.0	75.4	72.8	84.0	84.5

Shaded cells correspond to percentages inferior to 80%. The '90', '180', '360', labels in the walking condition column indicate turning trials of amplitudes: quarter turn (90°), half turn (180°) and full turn (360°), respectively. Similarly, the 'I', 'M' and 'E' labels indicate the stages of the turns: initiation, middle and end, respectively.

percentages, with drops below 80% for some conditions and groups. Figs. 2 and 3, which report typical kinematic signals for straight-line and full turn trials side-by-side, stress the degradation of some kinematic features when walking following a curved rather than a straight path. These Figures therefore illustrate the difficulties faced by the eight unsuitable features to detect gait events during turning trials.

Over all trials, the accuracies and precisions for HS detection were -0.47 and 1.09 frames for *O'Connor*, -4.43 and 1.46 frames for *Zeni*, and -1.36 and 3.53 frames for *Desailly*, respectively (1 frame @ 120 Hz = 8.3 ms). While the time errors significantly differed among groups and walking conditions for the three features (unreported results), more than 96% of accuracy and precision variations around the overall values were below 1 frame for *O'Connor* and *Zeni* (Table 3). Accuracies and precisions were less consistent among groups and walking conditions for *Desailly*, with variations

up to 10 frames. Comparing the features two-by-two turned at the advantage of *O'Connor*. Indeed, it reported better accuracies than *Zeni* in 97% of the cases (accuracies were never worse with *O'Connor*), and better precisions in 23% of the cases (precisions were worse in 3% of the cases). Accuracies and precisions were better with *O'Connor* than *Desailly* in 93% and 90% of the cases, respectively (accuracies and precisions were never worse with *O'Connor*). Differences between *Zeni* and *Desailly* were less distinct and consistent, as *Desailly* reported better accuracies in 57% of the cases (accuracies were worse in 3% of the cases with *Desailly*), and *Zeni* better precisions in 60% of the cases (precisions were never worse with *Zeni*).

Regarding TO detection, the overall accuracies and precisions were -3.44 and 1.50 frames for *O'Connor*, -0.93 and 1.28 frames for *Zeni*, and -1.02 and 2.18 frames for *Desailly*, respectively. Although the groups and walking conditions significantly affected

Table 3
Accuracies and precisions of *O'Connor*, *Zeni* and *Desailly* features for HS detection.

Group	Walking condition	Numerical values						Two-by-two method comparisons					
		<i>O'Connor</i>		<i>Zeni</i>		<i>Desailly</i>		Comparisons of accuracies			Comparisons of precisions		
		Accuracy	Precision	Accuracy	Precision	Accuracy	Precision	<i>O'Connor</i> Vs <i>Zeni</i>	<i>O'Connor</i> Vs <i>Desailly</i>	<i>Zeni</i> Vs <i>Desailly</i>	<i>O'Connor</i> Vs <i>Zeni</i>	<i>O'Connor</i> Vs <i>Desailly</i>	<i>Zeni</i> Vs <i>Desailly</i>
Young normal walking speed	Straight-line	-0.44 [#]	0.71 [#]	-4.41 [§]	0.90	-3.41 ^{§*}	1.14 [§]	<i>O'Connor</i>	<i>O'Connor</i>	<i>Desailly</i>	-	<i>O'Connor</i>	-
	90-I	-0.24 [#]	0.67 [#]	-3.93 [§]	0.87 [#]	-2.47 ^{§*}	1.40 ^{§*}	<i>O'Connor</i>	<i>O'Connor</i>	<i>Desailly</i>	-	<i>O'Connor</i>	<i>Zeni</i>
	90-M	-0.90 [#]	0.94	-4.40 [§]	0.99	-4.17 [§]	1.40	<i>O'Connor</i>	<i>O'Connor</i>	-	-	-	-
	90-E	-0.36 [#]	1.06 [#]	-4.83 [§]	1.12 [#]	-3.96 [§]	3.13 ^{§*}	<i>O'Connor</i>	<i>O'Connor</i>	-	-	<i>O'Connor</i>	<i>Zeni</i>
	180-I	-0.45 [#]	0.85 [#]	-4.12 [§]	0.96	-1.38 ^{§*}	1.41 [§]	<i>O'Connor</i>	<i>O'Connor</i>	<i>Desailly</i>	-	<i>O'Connor</i>	-
	180-M	-1.15 [#]	1.01 [#]	-4.50 [§]	1.53 [#]	-4.88 [§]	4.68 ^{§*}	<i>O'Connor</i>	<i>O'Connor</i>	-	-	<i>O'Connor</i>	<i>Zeni</i>
	180-E	0.33 [#]	1.01 [#]	-3.76 [§]	1.59 [#]	2.00 ^{§*}	2.72 ^{§*}	<i>O'Connor</i>	<i>O'Connor</i>	∅	-	<i>O'Connor</i>	<i>Zeni</i>
	360-I	-0.30 [#]	0.88	-4.17 [§]	0.96	-1.70 ^{§*}	1.27	<i>O'Connor</i>	<i>O'Connor</i>	<i>Desailly</i>	-	-	-
	360-M	-0.96 [#]	1.18 [#]	-4.34 [§]	1.43 [#]	6.94 ^{§*}	12.49 ^{§*}	<i>O'Connor</i>	<i>O'Connor</i>	<i>Zeni</i>	-	<i>O'Connor</i>	<i>Zeni</i>
	360-E	0.11 [#]	1.01 [#]	-3.72 [§]	1.47	-1.12 ^{§*}	1.73	<i>O'Connor</i>	<i>O'Connor</i>	<i>Desailly</i>	-	<i>O'Connor</i>	-
Young slower walking speed	Straight-line	-0.73 [#]	0.91 [#]	-5.13 [§]	1.38	-4.10 ^{§*}	1.52 [§]	<i>O'Connor</i>	<i>O'Connor</i>	<i>Desailly</i>	-	<i>O'Connor</i>	-
	90-I	-1.01 [#]	1.12 [#]	-5.36 [§]	1.80 [§]	-3.38 ^{§*}	2.72 [§]	<i>O'Connor</i>	<i>O'Connor</i>	<i>Desailly</i>	<i>O'Connor</i>	<i>O'Connor</i>	-
	90-M	-0.93 [#]	0.96 [#]	-4.82 [§]	1.34 [#]	-4.19 [§]	2.20 ^{§*}	<i>O'Connor</i>	<i>O'Connor</i>	-	-	<i>O'Connor</i>	<i>Zeni</i>
	90-E	-0.32 [#]	0.97 [#]	-5.65 [§]	1.78 [§]	-3.82 ^{§*}	2.46 [§]	<i>O'Connor</i>	<i>O'Connor</i>	<i>Desailly</i>	<i>O'Connor</i>	<i>O'Connor</i>	-
	180-I	-0.77 [#]	1.00 [#]	-4.90 [§]	1.09 [#]	-1.87 ^{§*}	2.12 ^{§*}	<i>O'Connor</i>	<i>O'Connor</i>	<i>Desailly</i>	-	<i>O'Connor</i>	<i>Zeni</i>
	180-M	-1.10 [#]	1.21 [#]	-5.46 [§]	1.73 [#]	-4.47 [§]	5.64 ^{§*}	<i>O'Connor</i>	<i>O'Connor</i>	-	-	<i>O'Connor</i>	<i>Zeni</i>
	180-E	-0.53 [#]	1.14 [#]	-5.55 [§]	1.79 [#]	1.23 [#]	4.12 ^{§*}	<i>O'Connor</i>	-	<i>Desailly</i>	<i>O'Connor</i>	<i>O'Connor</i>	<i>Zeni</i>
	360-I	-0.76 [#]	0.75 [#]	-4.75 [§]	1.30 [#]	-2.29 ^{§*}	2.15 ^{§*}	<i>O'Connor</i>	<i>O'Connor</i>	<i>Desailly</i>	<i>O'Connor</i>	<i>O'Connor</i>	<i>Zeni</i>
	360-M	-0.88 [#]	1.19 [#]	-4.84 [§]	1.74 [#]	5.93 ^{§*}	13.60 ^{§*}	<i>O'Connor</i>	<i>O'Connor</i>	<i>Zeni</i>	-	<i>O'Connor</i>	<i>Zeni</i>
	360-E	-0.18 [#]	1.06 [#]	-4.74 [§]	1.97 [§]	-2.15 ^{§*}	1.96 [§]	<i>O'Connor</i>	<i>O'Connor</i>	<i>Desailly</i>	<i>O'Connor</i>	<i>O'Connor</i>	-
Elderly normal walking speed	Straight-line	0.00 [#]	0.93 [#]	-4.10 [§]	1.16	-3.14 ^{§*}	1.62 [§]	<i>O'Connor</i>	<i>O'Connor</i>	<i>Desailly</i>	-	<i>O'Connor</i>	-
	90-I	-0.08 [#]	0.94 [#]	-4.02 [§]	1.55 [§]	-2.02 ^{§*}	2.44 [§]	<i>O'Connor</i>	<i>O'Connor</i>	<i>Desailly</i>	<i>O'Connor</i>	<i>O'Connor</i>	-
	90-M	0.01 [#]	1.38	-3.86 [§]	1.98	-3.26 ^{§*}	2.16	<i>O'Connor</i>	<i>O'Connor</i>	∅	-	-	-
	90-E	0.03 [#]	1.47 [#]	-3.91 [§]	2.02 [#]	-1.97 ^{§*}	3.31 ^{§*}	<i>O'Connor</i>	<i>O'Connor</i>	∅	-	<i>O'Connor</i>	<i>Zeni</i>
	180-I	-0.37 [#]	0.96 [#]	-4.17 [§]	1.29 [#]	-1.70 ^{§*}	2.30 ^{§*}	<i>O'Connor</i>	<i>O'Connor</i>	<i>Desailly</i>	-	<i>O'Connor</i>	<i>Zeni</i>
	180-M	-1.28	3.04 [#]	-3.71	1.79 [§]	-2.74	5.82 ^{§*}	-	-	-	<i>Zeni</i>	<i>O'Connor</i>	<i>Zeni</i>
	180-E	-0.12 [#]	1.57 [#]	-4.01 [§]	2.05 [#]	2.82 ^{§*}	4.00 ^{§*}	<i>O'Connor</i>	<i>O'Connor</i>	∅	-	<i>O'Connor</i>	<i>Zeni</i>
	360-I	-0.20 [#]	0.86 [#]	-4.09 [§]	1.28 [#]	-1.17 ^{§*}	2.23 ^{§*}	<i>O'Connor</i>	<i>O'Connor</i>	<i>Desailly</i>	-	<i>O'Connor</i>	<i>Zeni</i>
	360-M	-0.64 [#]	0.91 [#]	-3.68 [§]	1.54 [#]	6.58 ^{§*}	9.53 ^{§*}	<i>O'Connor</i>	<i>O'Connor</i>	∅	<i>O'Connor</i>	<i>O'Connor</i>	<i>Zeni</i>
	360-E	0.23 [#]	1.14 [#]	-3.97 [§]	1.41 [#]	-0.97 ^{§*}	2.58 ^{§*}	<i>O'Connor</i>	<i>O'Connor</i>	<i>Desailly</i>	-	<i>O'Connor</i>	<i>Zeni</i>

Differences among methods are reported as follow:

For an easier reading, the right part of the Table presents the comparison of the methods two-by-two. In this part, either the method with the better accuracy or precision (of the two) is reported, or a symbol is used to indicate that the methods are not different (-) or that neither method is better (∅).

The '90', '180', '360', labels in the walking condition column indicate turning trials of amplitudes: quarter turn (90°), half turn (180°) and full turn (360°), respectively. Similarly, the 'I', 'M' and 'E' labels indicate the stages of the turns: initiation, middle and end, respectively.

Numerical values are reported in frames, with 1 frame = 8.3 ms (120 Hz).

§ = different from *O'Connor* ($p < 0.017$).

* = different from *Zeni* ($p < 0.017$).

= different from *Desailly* ($p < 0.017$).

the time errors for the three methods (unreported results), accuracy and precision variations around the overall values were below 1 frame for *Zeni* (Table 4). Variations for *O'Connor* precision were also below 1 frame, whereas *O'Connor* accuracies and *Desailly* accuracies and precisions varied by up to 3 frames around the overall values. Comparing the features two-by-two turned at the advantage of *Zeni*. Specifically, accuracies and precisions were better with *Zeni* than *O'Connor* in 97% and 3% of the cases (accuracies and precisions were never worse with *Zeni*). Next, *Zeni* showed better accuracies and precisions than *Desailly* in 6% and 47% of the cases (accuracies and precisions were never worse with *Zeni*). Differences between *O'Connor* and *Desailly* were balanced, with *Desailly* reporting better accuracies in 63% of the cases (accuracies were never worse with *Desailly*) and *O'Connor* better precisions in 40% of the cases (precisions were worse in 3% of the cases with *O'Connor*).

4. Discussion

Analyzing the detection percentages confirmed that various features of foot marker trajectories can be used to detect HS and TO during straight-line walking. However, only *O'Connor*, *Zeni* and

Desailly features were able to detect HS and TO with detection percentages above 80% during straight-line walking and turning maneuvers for the three groups. These features had even overall detection percentage above 99%. Interestingly, these features are not drastically different from the other eight features found unsuitable to turning analysis (Ghoussayni et al., 2004; Hreljac and Marshall 2000; Hsue et al., 2007; Salazar-Torres, 2006). These observations therefore nicely highlight the value of the present study, as it would have been difficult identifying the most relevant features to analyze turning paths without testing them experimentally.

Comparing the time errors of the six features capable of adequately detecting HS or TO during straight and curved paths, confirmed prior works on straight-line walking suggesting that the detection could be improved by combining features among original publications (Bruening and Ridge, 2014; Hendershot et al., 2016). Specifically, the best results were obtained using *O'Connor* for HS and *Zeni* for TO. This observation is all the more important as Hendershot et al. (2016) recommended the same combination for straight-line walking. With this selection of features, HS and TO were detected with an average precision of 1.2 (range: 0.7 to 1.7)

Table 4
Accuracies and precisions of *O'Connor*, *Zeni* and *Desailly* features for TO detection.

Group	Walking condition	Numerical values						Two-by-two method comparisons					
		<i>O'Connor</i>		<i>Zeni</i>		<i>Desailly</i>		Comparisons of accuracies			Comparisons of precisions		
		Accuracy	Precision	Accuracy	Precision	Accuracy	Precision	<i>O'Connor</i> Vs <i>Zeni</i>	<i>O'Connor</i> Vs <i>Desailly</i>	<i>Zeni</i> Vs <i>Desailly</i>	<i>O'Connor</i> Vs <i>Zeni</i>	<i>O'Connor</i> Vs <i>Desailly</i>	<i>Zeni</i> Vs <i>Desailly</i>
Young normal walking speed	Straight-line	-2.38**	1.13	-0.51 [§]	1.16	-0.68 [§]	1.03	<i>Zeni</i>	<i>Desailly</i>	-	-	-	-
	90-I	-2.74**	1.43 [#]	-0.77 ^{§#}	1.28 [#]	0.63 ^{§*}	2.28 ^{§*}	<i>Zeni</i>	∅	∅	-	<i>O'Connor</i>	<i>Zeni</i>
	90-M	-2.65**	1.17 [#]	-0.78 [§]	1.03 [#]	-0.32 [§]	1.88 ^{§*}	<i>Zeni</i>	<i>Desailly</i>	-	-	<i>O'Connor</i>	<i>Zeni</i>
	90-E	-2.74**	1.14	-0.74 [§]	0.94	-0.51 [§]	1.38	<i>Zeni</i>	<i>Desailly</i>	-	-	-	-
	180-I	-2.89**	1.48 [#]	-0.79 [§]	1.18 [#]	-0.69 [§]	2.68 ^{§*}	<i>Zeni</i>	∅	-	-	<i>O'Connor</i>	<i>Zeni</i>
	180-M	-2.66**	1.69	-1.09 [§]	1.37	-1.06 [§]	2.42	<i>Zeni</i>	∅	-	-	-	<i>Zeni</i>
	180-E	-2.31**	0.85	-0.74 ^{§#}	0.90	-0.11 ^{§*}	1.08	<i>Zeni</i>	<i>Desailly</i>	∅	-	-	-
	360-I	-3.31**	1.21 [#]	-1.34 [§]	1.47 [#]	-1.14 [§]	2.49 ^{§*}	<i>Zeni</i>	<i>Desailly</i>	-	-	<i>O'Connor</i>	<i>Zeni</i>
	360-M	-3.49*	1.67 [#]	-1.38 ^{§#}	1.37 [#]	-2.90*	3.23 ^{§*}	<i>Zeni</i>	-	∅	-	<i>O'Connor</i>	<i>Zeni</i>
	360-E	-2.52**	1.43	-0.62 [§]	0.95	-0.79 [§]	1.25	<i>Zeni</i>	<i>Desailly</i>	-	-	-	-
Young slower walking speed	Straight-line	-2.40**	1.42	-0.47 [§]	1.17	-0.57 [§]	1.19	<i>Zeni</i>	<i>Desailly</i>	-	-	-	-
	90-I	-2.69**	1.32 [#]	-0.52 ^{§#}	1.40 [#]	0.58 ^{§*}	2.31 ^{§*}	<i>Zeni</i>	∅	∅	-	<i>O'Connor</i>	<i>Zeni</i>
	90-M	-2.42**	2.07	-0.85 [§]	1.44	-0.55 [§]	2.01	<i>Zeni</i>	<i>Desailly</i>	-	-	-	-
	90-E	-2.95**	1.74	-0.55 [§]	1.29	-0.15 [§]	1.56	<i>Zeni</i>	<i>Desailly</i>	-	-	-	-
	180-I	-2.92*	1.74 [#]	-1.05 [§]	1.48 [#]	-1.35	3.80 ^{§*}	<i>Zeni</i>	-	-	-	<i>O'Connor</i>	<i>Zeni</i>
	180-M	-2.69**	1.75	-1.09 ^{§#}	1.69	-0.12 ^{§*}	2.31	<i>Zeni</i>	∅	∅	-	-	-
	180-E	-2.71**	1.54 [#]	-0.71 ^{§#}	1.10	-0.14 ^{§*}	0.97 [§]	<i>Zeni</i>	<i>Desailly</i>	∅	-	<i>Desailly</i>	-
	360-I	-3.14	1.75 [#]	-1.54	1.27 [#]	-2.24	4.23 ^{§*}	-	-	-	-	<i>O'Connor</i>	<i>Zeni</i>
	360-M	-2.80*	2.05**	-1.03 ^{§#}	1.23 ^{§#}	-4.16*	4.20 ^{§*}	<i>Zeni</i>	-	<i>Zeni</i>	<i>Zeni</i>	<i>O'Connor</i>	<i>Zeni</i>
	360-E	-2.49**	1.22	-0.63 [§]	1.46	-0.79 [§]	1.51	<i>Zeni</i>	<i>Desailly</i>	-	-	-	-
Elderly normal walking speed	Straight-line	-4.37**	1.39	-1.14 [§]	0.95	-1.07 [§]	1.11	<i>Zeni</i>	<i>Desailly</i>	-	-	-	-
	90-I	-5.20**	1.39	-0.80 [§]	1.19	-0.23 [§]	1.70	<i>Zeni</i>	<i>Desailly</i>	-	-	-	-
	90-M	-4.01**	2.12	-0.98 [§]	1.33	-0.64 [§]	1.84	<i>Zeni</i>	<i>Desailly</i>	-	-	-	-
	90-E	-4.67**	1.36	-1.40 [§]	1.22	-1.17 [§]	1.54	<i>Zeni</i>	<i>Desailly</i>	-	-	-	-
	180-I	-5.14**	1.54 [#]	-1.37 [§]	1.17 [#]	-1.47 [§]	2.73 ^{§*}	<i>Zeni</i>	<i>Desailly</i>	-	-	<i>O'Connor</i>	<i>Zeni</i>
	180-M	-5.03**	1.73 [#]	-0.16 ^{§#}	1.69 [#]	-2.59 ^{§*}	3.54 ^{§*}	<i>Zeni</i>	∅	-	-	<i>O'Connor</i>	<i>Zeni</i>
	180-E	-4.44**	1.55	-0.84 [§]	1.39	-0.84 [§]	2.11	<i>Zeni</i>	<i>Desailly</i>	-	-	-	-
	360-I	-5.61**	1.36	-1.21 [§]	0.91 [#]	-1.28 [§]	1.94*	<i>Zeni</i>	<i>Desailly</i>	-	-	-	<i>Zeni</i>
	360-M	-5.15**	1.21 [#]	-0.78 ^{§#}	1.46 [#]	-3.32 ^{§*}	3.56 ^{§*}	<i>Zeni</i>	∅	<i>Zeni</i>	-	<i>O'Connor</i>	<i>Zeni</i>
	360-E	-4.67**	1.48	-0.84 [§]	1.24	-0.97 [§]	1.58	<i>Zeni</i>	<i>Desailly</i>	-	-	-	-

Legend is similar to Table 3.

frames for all walking conditions, except for the middle stage of the elderly group during half-turn, where the HS precision was 3.0 frames. While the paucity of temporal data regarding turning biomechanics in literature makes it difficult to assure that these precisions will be sufficient for future applications in research and clinical practice, it is worth mentioning that 1.2 and 3.0 frames, on average, correspond to only 1.3% and 3.3% of the stance durations recorded in this study during turning. Additionally, the precisions were smaller than most of the differences in stance duration observed between the young and elderly participants turning at normal speed, which ranged between 3 and 10 frames. Using *O'Connor* HS and *Zeni* TO features resulted in events detected on average 0.7 frames too early (range: -1.5 to 0.3). While such slight offsets in the detections should not be a concern for a majority of future applications, it remains possible calibrating the methods to suppress these systematic errors. Another important point to discuss is that using *O'Connor* to detect HS and *Zeni* to detect TO strongly reduces the importance of the ANOVAs' results regarding the variations in time errors among groups and walking conditions. In fact, while there were statistically significant variations among groups and conditions with *O'Connor* HS and *Zeni* TO features, a large majority of the variations were of less than 1.0 frame. Consequently, combining *Zeni* and *O'Connor* features led to variations among groups and walking conditions that are certainly small enough to be considered negligible for most applications.

The kinematic signals used by *Zeni* presented consistent triangular patterns whatever the group or the walking condition (Figs. 2

and 3). Therefore, detecting the global minimum and maximum peaks associated with HS and TO does not require too much computing and ensure a detection of all the events. The kinematics signals for *O'Connor* were also consistent among group and walking conditions. However, since the feature associated with HS is a local minimum peak, it was more difficult to detect automatically. Consequently, for HS, it could be useful first detecting the event occurrences using *Zeni* feature, and then determining the exact time of the events using *O'Connor* feature. This approach would allow detection percentages of 100% for both events, while maintaining the better accuracies and precisions obtained by combining *O'Connor* and *Zeni* features.

There is a practical difference between *O'Connor* and *Zeni* that could influence the choice of the method. In fact, with *Zeni* markers should be attached to the pelvis in addition to the feet, whereas *O'Connor* only requires foot markers. This difference remains for both straight-line and turning maneuvers analyses. The necessity to have markers on the pelvis could be an obstacle with some individuals (for example, obese persons) and motion capture system of limited capacity. However, pelvis markers are often included in gait analysis markers sets. Therefore, the need for pelvis markers should not be a major obstacle in future applications. In this study, we calculated the pelvis trajectory using four common markers in gait analysis, but it is possible that other and/or less markers could lead to comparable results. For example, placing the heel markers on lateral side instead of on the posterior side of the calcaneus lead to comparable results (Supplementary Materials).

There are a few other methodological points that are worth discussing. First, while the number of participants was limited, the repeated-measure dataset of almost 900 trials fully matched the study objectives. Second, although the observations were consistent among groups, further assessments could be necessary with severely pathological gait. In fact, prior research on straight-line walking recommended the same combination of *O'Connor* and *Zeni* features for uninjured subjects and transtibial amputees (Hendershot et al., 2016), but different features were advocated in more challenging gait patterns, such as cerebral palsy (Bruening and Ridge, 2014). Third, while the detections were supervised by an operator, it is possible that some events have been wrongly detected, especially for the kinematic signals that were strongly degraded during turning. However, this should not affect the study conclusions as the probability of incorrect detections mainly concerns features that are incompatible with turning anyway. Fourth, we cannot exclude that other features could provide better results. Fifth, this study analyzed detection percentages, accuracies and precisions. However, other performances could be important, such as suitability for real-time detection or sampling frequency requirement. Sixth, the results may be different when wearing shoes. Finally, while this study focused on detecting gait events using motion capture systems, other technologies exist, such as pressure insoles (Rouhani et al., 2011).

In conclusion, this study extended straight-line detection methods and identified a preferable combination of features, *O'Connor* HS and *Zeni* TO, to analyze turning in young and elderly adults even when the participants walk with short steps. Overall, this combination allowed detection percentages above 99%, accuracy below 1.0 frame and precision below 1.5 frames. It also showed relatively small variations among groups and walking conditions. Interestingly, the same combination was previously recommended to analyze straight-line walking of healthy individuals and patients with moderate gait pathology (Hendershot et al., 2016), suggesting that it could be suitable to detect gait events in these populations for any type of straight and curved paths.

Acknowledgement

This study was partially funded by the Swiss National Science Foundation (SNSF grant #32003B-166433) and the Profectus foundation. The study sponsors were not involved in the study design, in the collection, analysis and interpretation of data, in the writing of the manuscript, and in the decision to submit the manuscript for publication. BMJ, DHB and JF supervised this study and should be considered as last authors.

Conflict of interest statement

The Authors confirm that none of the Authors has any conflict of interest regarding the work presented in this manuscript and that the sources of funding, which had no influence on this research, are cited properly in the manuscript.

Appendix A. Supplementary material

Supplementary data to this article can be found online at <https://doi.org/10.1016/j.jbiomech.2019.05.006>.

References

Akram, S.B., Frank, J.S., Chenouri, S., 2010. Turning behavior in healthy older adults: is there a preference for step versus spin turns? *Gait & Posture* 31, 23–26.
 Barrios, J.A., Crossley, K.M., Davis, I.S., 2010. Gait retraining to reduce the knee adduction moment through real-time visual feedback of dynamic knee alignment. *J. Biomech.* 43, 2208–2213.

Bennour, S., Ulrich, B., Legrand, T., Jolles, B.M., Favre, J., 2018. A gait retraining system using augmented-reality to modify footprint parameters: Effects on lower-limb sagittal-plane kinematics. *J. Biomech.* 66, 26–35.
 Bhatt, H., Pieruccini-Faria, F., Almeida, Q.J., 2013. Dynamics of turning sharpness influences freezing of gait in Parkinson's disease. *Parkinsonism Related Disorders* 19, 181–185.
 Bloem, B.R., Grimbergen, Y.A.M., Cramer, M., Willemsen, M., Zwinderman, A.H., 2001. Prospective assessment of falls in Parkinson's disease. *J. Neurol.* 248, 950–958.
 Bourgeois, A.B., Mariani, B., Aminian, K., Zambelli, P.Y., Newman, C.J., 2014. Spatio-temporal gait analysis in children with cerebral palsy using, foot-worn inertial sensors. *Gait & Posture* 39, 436–442.
 Bovonsunthonchai, S., Hiengkaew, V., Vachalathiti, R., Said, C.M., Batchelor, F., 2015. Temporospacial analysis: gait characteristics of young adults and the elderly in turning while walking. *International J. Therapy Rehabil.* 22, 129–134.
 Bruening, D.A., Ridge, S.T., 2014. Automated event detection algorithms in pathological gait. *Gait & Posture* 39, 472–477.
 Crenna, P., Carpinella, I., Rabuffetti, M., Calabrese, E., Mazzoleni, P., Nemni, R., Ferrarin, M., 2007. The association between impaired turning and normal straight walking in Parkinson's disease. *Gait & Posture* 26, 172–178.
 Cumming, R.G., Klineberg, R.J., 1994. Fall frequency and characteristics and the risk of hip fractures. *J. Am. Geriatr. Soc.* 42, 774–778.
 Desailly, E., Daniel, Y., Sardain, P., Lacouture, P., 2009. Foot contact event detection using kinematic data in cerebral palsy children and normal adults gait. *Gait & Posture* 29, 76–80.
 Dixon, P.C., Stebbins, J., Theologis, T., Zavatsky, A.B., 2016. The use of turning tasks in clinical gait analysis for children with cerebral palsy. *Clin. Biomech.* 32, 286–294.
 Favre, J., Erhart-Hledik, J.C., Chehab, E.F., Andriacchi, T.P., 2016. General scheme to reduce the knee adduction moment by modifying a combination of gait variables. *J. Orthop. Res.* 34, 1547–1556.
 Ghousayni, S., Stevens, C., Durham, S., Ewins, D., 2004. Assessment and validation of a simple automated method for the detection of gait events and intervals. *Gait & Posture* 20, 266–272.
 Giladi, N., McMahon, D., Przedborski, S., Flaster, E., Guillery, S., Kostic, V., Fahn, S., 1992. Motor blocks in Parkinson's disease. *Neurology* 42, 333.
 Glaister, B.C., Bernatz, G.C., Klute, G.K., Orendurff, M.S., 2007. Video task analysis of turning during activities of daily living. *Gait & Posture* 25, 289–294.
 Hendershot, B.D., Mahon, C.E., Pruziner, A.L., 2016. A comparison of kinematic-based gait event detection methods in a self-paced treadmill application. *J. Biomech.* 49, 4146–4149.
 Hreljac, A., Marshall, R.N., 2000. Algorithms to determine event timing during normal walking using kinematic data. *J. Biomech.* 33, 783–786.
 Hreljac, A., Stergiou, N., 2000. Phase determination during normal running using kinematic data. *Med. Biol. Eng. Compu.* 38, 503–506.
 Hsue, B.J., Miller, F., Su, F.C., Henley, J., Church, C., 2007. Gait timing event determination using kinematic data for the toe walking children with cerebral palsy. *J. Biomech.* 40, S529.
 Huxham, F., Gong, J., Baker, R., Morris, M., Iansek, R., 2006. Defining spatial parameters for non-linear walking. *Gait & Posture* 23, 159–163.
 Mellone, S., Mancini, M., King, L.A., Horak, F.B., Chiari, L., 2016. The quality of turning in Parkinson's disease: a compensatory strategy to prevent postural instability? *J. Neuroeng. Rehabil.* 13, 39.
 O'Connor, C.M., Thorpe, S.K., O'Malley, M.J., Vaughan, C.L., 2007. Automatic detection of gait events using kinematic data. *Gait & Posture* 25, 469–474.
 Orendurff, M.S., Segal, A.D., Berge, J.S., Flick, K.C., Spanier, D., Klute, G.K., 2006. The kinematics and kinetics of turning: limb asymmetries associated with walking a circular path. *Gait & Posture* 23, 106–111.
 Rouhani, H., Crevoisier, X., Favre, J., Aminian, K., 2011. Outcome evaluation of ankle osteoarthritis treatments: plantar pressure analysis during relatively long-distance walking. *Clin. Biomech.* 26, 397–404.
 Salazar-Torres, J.-J., 2006. Validity of an automated gait event detection algorithm in children with cerebral palsy and non-impaired children. *Gait & Posture* 24, S130–S131.
 Schaafsma, J.D., Balash, Y., Gurevich, T., Bartels, A.L., Hausdorff, J.M., Giladi, N., 2003. Characterization of freezing of gait subtypes and the response of each to levodopa in Parkinson's disease. *Eur. J. Neurol.* 10, 391–398.
 Strike, S.C., Taylor, M.J.D., 2009. The temporal-spatial and ground reaction impulses of turning gait: is turning symmetrical? *Gait & Posture* 29, 597–602.
 Taylor, M.J.D., Dabnicki, P., Strike, S.C., 2005. A three-dimensional biomechanical comparison between turning strategies during the stance phase of walking. *Hum. Mov. Sci.* 24, 558–573.
 Thigpen, M.T., Light, K.E., Creel, G.L., Flynn, S.M., 2000. Turning difficulty characteristics of adults aged 65 years or older. *Phys. Ther.* 80, 1174–1187.
 Tinetti, M.E., Speechley, M., Ginter, S.F., 1988. Risk factors for falls among elderly persons living in the community. *N. Engl. J. Med.* 319, 1701–1707.
 Wood, B.H., Biclough, J.A., Bowron, A., Walker, R.W., 2002. Incidence and prediction of falls in Parkinson's disease: a prospective multidisciplinary study. *J. Neurol. Neurosurg. Psychiatry* 72, 721–725.
 Zeni, J.A., Richards, J.G., Higginson, J.S., 2008. Two simple methods for determining gait events during treadmill and overground walking using kinematic data. *Gait & Posture* 27, 710–714.
 Zeni, J.A., Higginson, J.S., 2010. Gait parameters and stride-to-stride variability during familiarization to walking on a split-belt treadmill. *Clin. Biomech.* 25, 383–386.